Separation and Capture of Circulating Tumor Cells from Whole Blood Using a Bypass Integrated Microfluidic Trap Array

[1]Yousang Yoon, [1]Sunki Cho, [1]Seonil Kim, [1]Eunsuk Choi, [2]Rae-Kwon Kim, [2]Su-Jae Lee, [3]Onejae Sul, and [1,3]Seung-Beck Lee*, *IEEE-Member*

***Abstract*— We report on a microfluidic trap array that separates and captures circulating tumor cells (CTCs) from whole blood. The device is a series array of microfluidic branches that utilizes the difference in flow rates between the bypass channel and the trap channel to allow CTCs in whole blood to be separated and trapped. Once a trap has captured a cell with diameter larger than the narrow trap outlet, additional cells arriving at the branch would flow towards the bypass channel due to its lower flow resistance. Results demonstrated that it was possible to capture CTCs from the whole blood of a mouse with full-blown metastasis. With further developments, the bypass integrated microfluidic trap array could become a useful tool for the early prognosis of cancer metastasis.**

I. Introduction

With the development of various biomedical techniques for early intervention, many types of early stage cancers are being cured. However, approximately 90% of cancer related organ malfunctions and deaths are caused by cancer metastasis rather than direct impact of the primary tumor [1-2]. Recent studies have revealed that the main cause for the spread of cancer was by circulating tumor cells (CTCs) which were derived from the primary tumor, circulating in the bloodstream, and relocating in distant organs creating tumors at secondary sites. For this reason, the number of CTCs in the blood may be a strong indicator for prognosis, therapeutic responses, and the patient's survivability [3]. Therefore, the enrichment, isolation and enumeration of CTCs have become important issues for the development of tailored treatment to increase life expectancy of cancer patients [4-6]. Enumerating CTCs in patients' blood, however, is very challenging due to their scarcity in early stage metastasis, few to less than 100 CTCs per 10^7 hemocytes at most [7].

Of the many methods developed for enumerating CTCs, microfluidic lab-on-a-chip techniques have been providing solutions to overcome this difficulty. Researchers have reported successful microfluidic devices capable of capturing and detecting CTCs from human blood with various platforms which can be divided into two categories: one is the selective binding of epithelial cell adhesion molecule (EpCAM) and the other is using the size difference of CTCs against normal hemocytes. EpCAM is frequently over expressed by carcinomas and coating anti-EpCAM antibodies on the device surface enabled CTCs to be successfully separated from whole blood [8-10]. However, down-regulated EpCAM expression caused by heterogeneity of CTCs makes anti-EpCAM based techniques less effective [11-12]. Alternatively, CTCs can be isolated using the fact that the size of CTCs is usually larger than other blood cells. This size-based technique can capture CTCs regardless of EpCAM expression and thus without antigen-antibody binding. The reduced use of reagents and human generated sample requires less analysis time and prevents the possibility of manipulation error. If not properly designed, however, size-based filtration may lead to serious inefficiencies. Trapped cells, of which most are leukocytes, can eventually clog the device causing cell loss [13-14]. Moreover, even successful systems overlook the need for single-cell capture of CTCs. Captured cells were all lumped together, which makes it hard to enumerate and analyze. The ability of precise enumeration of CTCs, which is essential for cancer prognosis, would make a device clinically valuable [15]. Tan and Takeuchi reported a hydrodynamic single bead trapping that depended on the ratio of the fluid fluxes of trap and bypass channels caused by the difference in fluidic resistance [16]. We applied this technique for the separation and capture of CTCs in whole blood. By optimizing the microfluidic channel dimensions for flow rate, pressure and CTC size, we were able to demonstrate separation and capture of individual CTCs from mice whole blood with high efficiency.

II. Concept of the Microfluidic Device

The microfluidic channel comprises of a straight channel with narrow trap sites and a branched bypass channel, as illustrated in figure 1, and the flow resistances of the two paths can be geometrically controlled according to the following equation:

$$\frac{\mathrm{Q_t}}{\mathrm{Q_b}} = \left(\frac{L_b}{L_t}\right)\left(\frac{W_b + H_b}{W_t + H_t}\right)^2 \left(\frac{W_t H_t}{W_b H_b}\right)^3 \quad (1)$$

where Q is volumetric flow rate, L is the channel length, W is the channel width, H is the channel height and the subscripts t and b refers to the path to a trap site and a bypass channel, respectively [16]. When a CTC flowing in the channel arrives at a branching point, the lower flow resistance of the trapping channel, compared to the bypass channel, induces it to be captured in the narrow trap site. This leads to an alteration in the flow resistance, and allows the following CTCs to proceed to the bypass channel, where the flow resistance has become lower than the trapping channel. The following CTCs will flow along to the next branching point where they will be led into the next trap site [16].

This research was supported by the Converging Research Center Program (Project No. 2013K000283) funded by the Ministry of Science, ICT & Future Planning, and the Basic Science Research Program (2013R1A1A2011532 & 2012R1A6A1029029) through the National Research Foundation of Korea (NRF) funded by the Ministry of Education.

[1]Department of Electronic Engineering, [2]Department of Life Science and Research Institute for Natural Sciences, [3]Institute of Nano Science and Technology, Hanyang Universtiy, 222 Wangsimni-ro, Seongdong-gu, Seoul 133-791, Korea (phone: 82-2-2220-1676; fax: 82-2-2294-1676; e-mail: sbl22@hanyang.ac.kr).

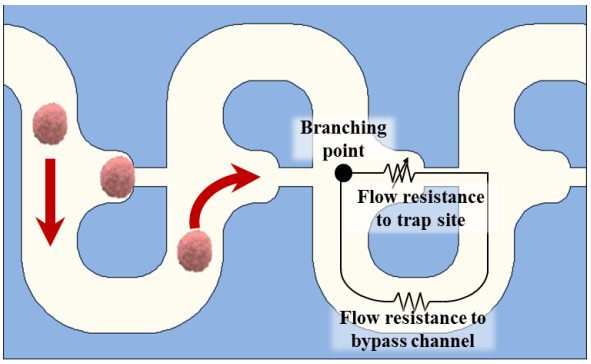

Figure 1. Conceptual image of a single cell capture in the bypass integrated microfluidic trap array

Considering that the reported sizes of the CTCs were between 15 µm to 27 µm, the width of the inlet and bypass channels were defined as 30 µm [17]. The trap sites, on the other hand, were designed to have a narrower width of 10 µm, which would capture target cells, while other hemocytes having smaller sizes and larger deformability would pass through. The height of the whole channel was designed to be 30 µm to minimize the possibility of more than one target cell being captured at the same site.

III. Materials and Methods

A. Fabrication Method

The microfluidic channels were fabricated on an oxidized 2 x 2 cm^2 silicon chip which provides the potential for future integration of various sensors on the same chip. To enhance adhesion between the SiO_2 surface and the SU-8 (2075, Microchem) optical resist, Surpass 3000 (Dischem) was spin coated followed by deionized water rinse. The SU-8, that forms the channel walls, had a thickness of 30 µm. The microfluidic channel pattern was defined by optical lithography. To seal the device, polydimethylsiloxane (PDMS, Dow corning) was used. To make the device free from leakage, the surface of the patterned SU-8 was treated with O_2 plasma (50 W, 160 mTorr, 30 s) resulting in a hydrophilic surface. It was then heated at 80°C in 5% (3-aminopropyl)triethoxysilane for 10 minutes to form amine groups (Si-NH_2) on the surface of SU-8. Performing the same O_2 plasma treatment on the PDMS allows Si-O-Si covalent bonds to form with the pretreated SU-8, resulting in a firm microfluidic channel which may endure high fluid pressures (see figure 2(a)). The fabricated device has 16 parallel microfluidic channels with each having 100 trap sites. The scanning electron microscope (SEM) image of the SU-8 fluidic channel walls and the narrow trap site is shown in figure 2(b). The optical image of the fabricated device can be seen in figure 2(c).

B. Simulation and Device Optimization

The fluid flow through two consecutive trap sites was studied using computer simulation (COMSOL Multiphysics) to study the hydrodynamic conditions of the device and optimize the device geometry for single-cell capture of CTCs. The simulation was performed under Ma < 0.3 and laminar flow condition. The volumetric flow rate, a critical factor for device operation, was calculated by surface integration of velocities for various conditions. Figure 3(a) and (b) show the velocity and the streamlines which are lines of velocity vector field before and after CTC capture with the width fixed at 30 µm. It can be seen in figure 3(a), that initially the fluid velocity is higher at the trap site which leads large cells toward the trap. Once a cell becomes trapped and partially blocks the trap outlet, the fluidic pressure increases allowing other flowing cells to flow toward the bypass channel. The initial flow rates of the bypass and trap channels can be controlled by their relative lengths (see figure3(c)). The capture efficiency representing the probability of a cell to be captured in a trap site was derived by the following equation:

$$P_c = \frac{1}{1+Q_b/Q_t} \quad (2)$$

where P_c is the probability of cell capture [18]. As the channel length gets longer, the volumetric flow rate to the trap site proportionally increases, which means a higher capture probability. We found that a Pc > 50 % can be achieved with Qb/Qt =1.1. The size variation and deformation of cells hinder captured cells from completely filling the trap site. If excessively long bypass channels are chosen, it may have too much of an initial flow rate difference and may not be effective at altering the major flow direction after a cell has been captured. When captured cells cannot completely fill the trap site, the fluid flux around the trapped cells may cause multiple cells to be captured at the same site. Also, high fluid flux around the trapped cell may apply too much pressure and cause cells to rupture. Through simulations based on CTC size distribution we found that a bypass channel with the width of 30 µm and the length of 450 µm would be advantageous for effective single cell capture and cell viability.

C. Sample Preparation

Human breast cancer cell line MDA-MB-231 was established from the American Type Culture Collection (Manassas, VA). Lung metastasized (LM) MDA-MB-231 cells were derived from MDA-MB-231 that was metastasized to lung in mice. These cells were grown in Dulbeco's modified eagle's medium supplemented with 10% fetal bovine serum, penicillin (100 units/ml), streptomycin (100 g/ml) and cultured in a humidified 5% CO_2 atmosphere at 37 °C. Whole

Figure 2. (a) Illustration of the microfluidic channel, (b) SEM image of the patterned SU-8 channel, (c) optical image of the fabricated device

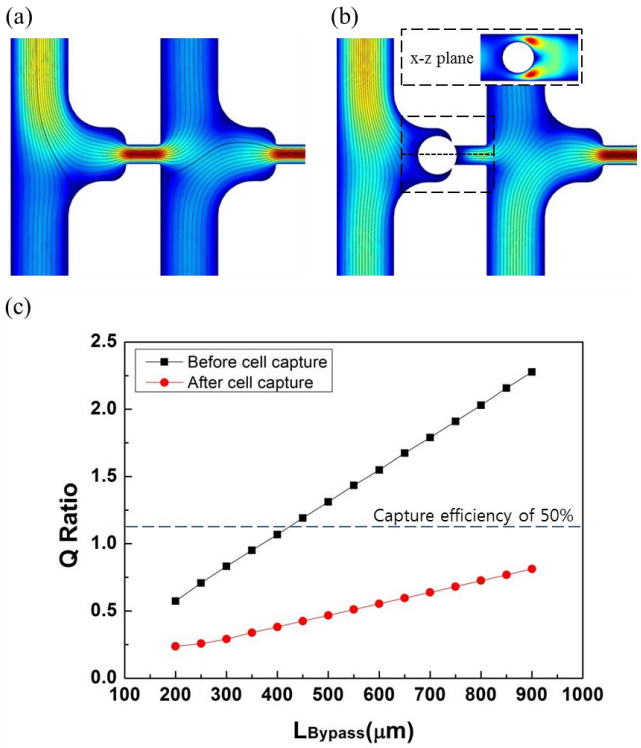

Figure 3. Simulated results varying the length of the bypass channel. (a) Velocity and streamlines before a cell capture and (b) after a cell capture. Inset (b) is a cross section (x-z plane) showing the velocity of fluid around a captured cell. (c) Volumetric flow rate ratio between the trapping channel and the bypass channel before and after cell capture.

blood which contained green fluorescent protein (gfp) tagged CTCs was drawn from mice with full-blown metastasis [19-20].

IV. Results and Discussion

Suspension of LM MDA-MB-231 cells in phosphate buffered saline (PBS) having a density of 100 cells/ml was prepared, and 1% F-127 (Sigma Aldrich) solution was injected for 10 minutes to prevent nonspecific cell adhesion prior to cell injection. 0.5 ml of the prepared cell suspension was drawn by a syringe (Becton Dickinson) and injected into the fabricated microfluidic device through syringe pump (Chemyx) with the flow rate of 1.6 ml/h. The microfluidic

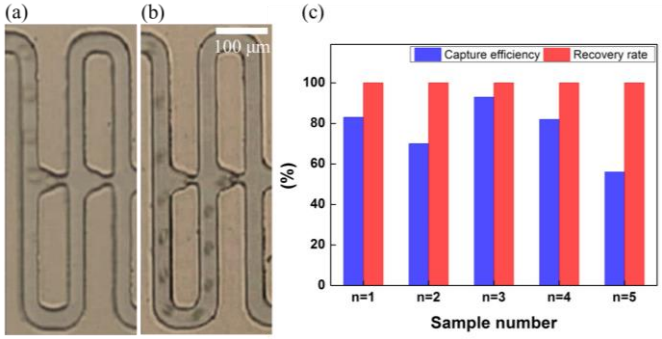

Figure 4. (a) The trajectory of a cell being captured to the first trap site. (b) The trajectory of a cell passing an occupied trap site and being captured at the following trap site. (c) Capture efficiency and recovery rate of five experiments using LM MDA-MB-231 cell line.

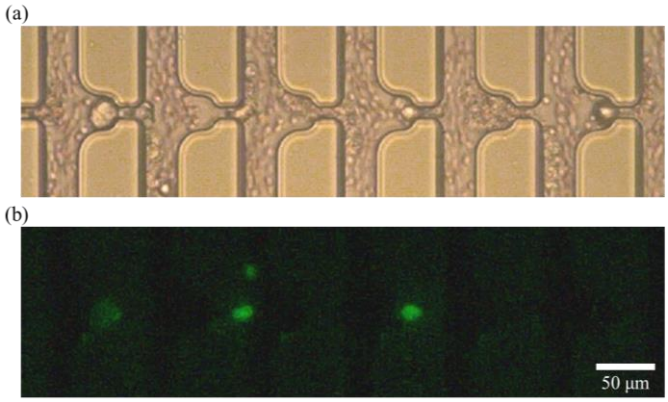

Figure 5. (a) Bright field microscopic image of captured cells from diluted mice blood. (b) Fluorescent image of captured CTCs with over-expressed gfp.

device was rinsed with PBS solution to collect possible remaining cells in the tube. Waste from the outlet during the whole process was collected on a clean petri dish, and the presence of any cells was verified optically. The experimental process was repeated 5 times.

Figure 4(a) shows the trajectory of a target cell trapped at the first trap site. Figure 4(b) is showing the trajectory of another cell, bypassing the trap site that already had a trapped cell, and proceeding to the next trap and become captured. Each of the 16 parallel fluidic channels had a fluid flow rate of 0.1 ml/h and the resulted in the hydraulic pressure applied to the captured cells being small enough to keep most of them in the trapping sites. The same pressure was big enough for most hemocytes, especially leukocytes, to squeeze through the trapping channel. Not all of the cells were trapped at the first trap site they encountered and empty traps were found. However, there were no cells found in the outlet waste, showing that all of the injected cells were eventually captured. By counting the empty trap sites up to the site of capture, the capture efficiency was estimated, at an average 76 %, and was found to be higher than the simulated result of 54 % (see figure 4(c)). The disagreement may be from the initial position of the cells relative to the channel walls which was not considered in the simulation. When a cell was positioned near the wall, more of the fluid around the cell was directed toward the trap site compared to cells positioned in the middle of the channel, leading to higher capture rates. We also found that very few trap sites were occupied by multiple cancer cells. This may be due to the deformation of the trapped cells blocking most of the flow through the trap site, which will result in a higher fluid resistance compared to the bypass channel then calculated. Considering that not a single cell was shown in the waste, we found that our microfluidic device was very efficient at capturing the injected target cells when their diameter was larger than the trap outlet.

We proceeded to apply the device for detection of CTCs from whole blood drawn from mice with full-blown cancer metastasis to verify whether the microfluidic trap array was capable of CTC capture in the presence of overwhelming numbers of erythrocytes and leukocytes. The blood sample was diluted with a PBS solution that had 8 times the volume. It can be seen in figure 5(a), that larger cells were trapped while

smaller erythrocytes flowed through the bypass and the trap channels. Since there are normally a thousand times more leukocytes than CTCs in whole blood, we may presume that most of the captured cells were leukocytes. The initial MDA-MB-231 cells used had their green fluorescent protein over expressed, which allowed the CTCs to be distinguished from leukocytes by using fluorescent imaging. It can be seen in figure 5(b) that the trapped cells were mostly CTCs with only few leukocytes. This may be due to the high deformability of the leukocytes making it possible for them to squeeze through the narrow 10 μm trap channel. Although there were some trap sites with multiple cells captured, it was shown that there was only a single CTC amongst them. The results demonstrate that it was possible to use the bypass integrated microfluidic trap array for separation and capture of CTCs from whole blood for enumeration and analysis. Some smaller CTCs were seen to be flowing much slower in the channel than other hemocytes which may have been the cause of the agglomeration of cells and channel blockage. This hindered quantitative analysis of the efficiency of the trap sites by causing channels to be blocked before the whole of the blood sample was passed through. Considering that there are 16 parallel channels, the device was able to accommodate some of the channels being blocked. However, further research is required to reduce channel blockage, which may be achieved by increasing the mobility of the CTCs by reducing their adhesion to the fluidic channel inner surfaces.

V. Conclusion

We have systematically optimized the device geometry and demonstrated the operation of a bypass integrated microfluidic trap array for the separation and capture of CTCs from whole blood. Using LM MDA-MB-231 cells, it was possible to achieve 56-93% capture efficiency for a single trap site. Using a series of consecutive trap sites, we demonstrated that complete recovery of cells above a specific size was possible. Also, we demonstrated the detection of CTCs from whole blood drawn from mice with full-blown metastasis showing that it was possible to use the bypass integrated microfluidic trap array for separation and capture of individual CTCs from whole blood for enumeration and analysis.

References

[1] P.Mehlen, "Metastasis: a question of life or death," Nat. Rev. Cancer, 6(6), 449-458, 2006.

[2] K.Pantel, "Circulating tumour cells in cancer patients: challenges and perspectives," Trends Mol. Med., 16(9), 398-406, 2010.

[3] A.Delacruz, "Using circulating tumor cells as a prognostic indicator in metastatic castration-resistant prostate cancer," Clin. J. Oncol. Nurs., 16(2), E44-E47, 2012

[4] M.Y.Kim, "Tumor Self-Seeding by Circulating Cancer Cells," Cell, 139(7), 1315-1326, 2009.

[5] Y.Dong, "Microfluidics and Circulating Tumor Cells," J. Mol. Diagn., 15(2), 149-157, 2012.

[6] M.Cristofanilli, "Circulating Tumor Cells, Disease Progression, and Survival in Metastatic Breast Cancer," N. Engl. J. Med., 351(8), 781-791, 2004.

[7] K.Hyun, "Advances and critical concerns with the microfluidic enrichments of circulating tumor cells," Lab Chip, 14(1), 45-56, 2014.

[8] S.Nagrath, "Isolation of rare circulating tumour cells in cancer patients by microchip technology," Nature, 450(7173), 1235-1239, 2007.

[9] S.L.Stott, "Isolation of circulating tumor cells using a microvortex-generating herringbone-chip," PNAS, 107(43), 18392-18397, 2010.

[10] H.J.Yoon, "Sensitive capture of circulating tumour cells by functionalized graphene oxide nanosheets," Nature Nanotechnology, 8(881), 735-741, 2013.

[11] J.D.Toonder, "Circulating tumor cells: the Grand Challenge," Lab Chip, 11(3), 375-377, 2011.

[12] T.M.Gorges, "Circulating tumour cells escape from EpCAMbased detection due to epithelial-tomesenchymal transition," BMC Cancer, 12, 178, 2012.

[13] S.Zheng, "Membrane microfilter device for selective capture, electrolysis and genomic analysis of human circulating tumor cells," J. Chromatogr. A, 1162(2), 154-161, 2007.

[14] H.K.Lin, "Portable Filter-Based Microdevice for Detection and Characterization of Circulating Tumor Cells," Clin Cancer Res, 16(20), 5011-5018, 2010.

[15] S.J.Tan, "Microdevice for the isolation and enumeration of cancer cells from blood," Biomed Microdevices, 11(4), 883-892, 2009.

[16] W.H.Tan, "A trap-and-release integrated microfluidic system for dynamic microarray applications," PNAS, 104(4), 1146-1151, 2007

[17] G.Vona, "Isolation by size of epithelial tumor cells a new method for the immunomorphological and molecular characterization of circulatingtumor cells," Am. J. Pathol., 156(1), 57-63, 2000

[18] J.H Chung, "Highly-efficient single-cell capture in microfluidic array chips using differential hydrodynamic guiding structures," Applied Physics Letters, 98, 123701, 2011

[19] A.J Minn, "Genes that mediate breast cancer metastasis to lung," Nature, 436, 518-524, 2005

[20] A.Fantozzi, "Mouse models of breast cancer metastasis," Breast Cancer Res, 8(4), 212-222, 2006